Iodide Electron Transfer Kinetics in Dye-Sensitized Nanocrystalline TiO_2 Films

Ivan Montanari,[†] Jenny Nelson,[‡] and James R. Durrant*[,†]

Departments of Chemistry and Physics, Centre for Electronic Materials and Devices, Imperial College of Science Technology and Medicine, London SW7 2AY, United Kingdom

Received: March 25, 2002

Electron transfer kinetics plays a key role in determining the energy conversion efficiency of dye-sensitized photoelectrochemical solar cells. Photoinduced charge separation in such cells results in oxidation of the sensitizer dye. The resulting dye cation may be rereduced by recombination with injected electrons or by electron transfer from iodide ions in the redox electrolyte, often referred to as the regeneration reaction. In this paper, we employ transient absorption spectroscopy to investigate the kinetic competition between these two pathways in $Ru(dcbpy)_2(NCS)_2$-sensitized nanocrystalline film TiO_2 electrodes immersed in a propylene carbonate electrolyte. The experiments monitored both the dye cation decay kinetics and the yield of product species, assigned to I_2^- radicals generated by electron transfer from iodide ions to the dye cation. The kinetic competition between the recombination and the regeneration processes is found to be dependent upon both the iodide concentration and the electrical bias applied to the dye-sensitized electrode. Similar regeneration kinetics were observed when Zn-tetra-p-carboxy-phenyl-porphyrin was used as sensitizer dye. In contrast to the recombination reaction, the rate of the dye cation regeneration reaction by iodide is found to be independent of applied bias. At high iodide concentrations, the cation regeneration reaction is sufficiently fast to compete successfully with the recombination reaction for all biases studied. When an intermediate iodide concentration is used, the acceleration of the recombination kinetics at negative biases results in a reduction in the dye cation lifetime and a loss of I_2^- yield. This bias dependence is found to be in good agreement with a numerical modeling of the data employing a continuous time random walk model for the charge recombination dynamics, assuming the iodide reaction to be first-order in iodide concentration. We conclude by discussing the implications of these observations for solar cell function.

Introduction

Dye-sensitized photoelectrochemical solar cells based on nanocrystalline metal oxide electrodes are a promising class of alternative photovoltaic systems. In such devices, the kinetics of electron transfer pathways at the metal oxide/sensitizer dye/electrolyte interface are critical to device function. Research is increasingly focusing on control of these interfacial electron transfer kinetics in order to optimize device function. Figure 1 summarizes those pathways of relevance to this paper. The electron injection process (k_{inj}) has been shown by various groups to take place on an ultrafast time scale[1−4] with at least three components spanning 10^{-13}−10^{-10} s. The charge recombination process (k_{CR}) between injected electrons and photogenerated dye cations has a strongly nonexponential behavior and spans several orders of magnitude.[5−7] This has been modeled in terms of electron diffusion within an exponential distribution of trap sites in the nanocrystalline electrode.[8,9] In this context, the competition between this "wasteful" charge recombination (k_{CR}) and the desired dye ground state regeneration by the redox electrolyte (k_{RG}) may play a role in determining device efficiency. In particular, we have recently shown that k_{CR} is strongly dependent upon the Fermi level of the TiO_2 electrode, indicating that depending upon device composition, this kinetic competition may be particularly significant as the cell voltage approaches open circuit.[5]

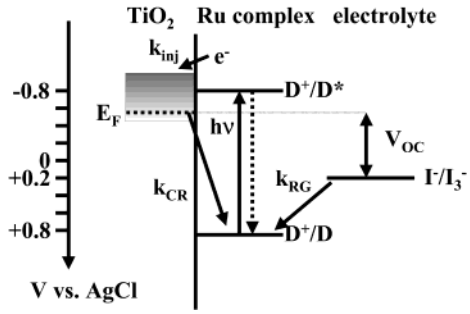

Figure 1. Schematic diagram showing the main interfacial electron steps involved in a dye-sensitized cell. k_{inj} is the electron injection step. k_{CR} represents the charge recombination between dye cations and electrons in the semiconductor while k_{RG} is the dye cation regeneration by a redox couple (I^-/I_3^-) in solution. V_{OC} is the open circuit voltage of the cell.

In dye-sensitized photoelectrochemical cells, an I^-/I_3^- redox couple in solution is typically employed to reduce the dye cation anchored on the surface of the semiconductor (k_{RG}) and to shuttle electrons from the counter electrode to the dye-sensitized electrode. Developing alternatives to the iodide/tri-iodide couple, including solid state electrolytes, is an active area of research[10,11] although device efficiencies remain relatively low to date. However, the parameters affecting the dye rereduction kinetics by I^- have received only limited attention to date,[12−16] hindering the modeling and optimization of devices employing this redox couple.

Studies of iodide rereduction of the dye cation are complicated by the fact that the I^-/I_3^- system is a two electron redox couple,

* To whom correspondence should be addressed. Fax: +44-20-7594 5801. E-mail: j.durrant@ic.ac.uk.
† Department of Chemistry.
‡ Department of Physics.

10.1021/jp025824c CCC: $22.00
Published on Web 11/06/2002

requiring the reaction to proceed through one or more intermediate states. Previous studies have largely addressed the iodide oxidation kinetics following UV excitation of TiO_2 colloidal particles.[17−19] Results obtained with $Ru(dcbpy)_3$-sensitized colloids in aqueous iodide have been interpreted in terms of the formation of an iodide−ruthenium(III) complex intermediate, enhancing the efficiency of this reaction.[12] In contrast, Kamat et al. have indicated that the kinetics of dye cation rereduction by iodide are approximately first-order for a small range of iodide concentrations with no evidence for complex formation.[13] In a study comparing nanocrystalline electrodes sensitized with ruthenium(II)$(dcbpy)_2(CN)_2$ dyes and their osmium analogues, the poor cell performance obtained with the osmium dyes was attributed to the "sluggishness" of the iodide rereduction reaction, resulting in significant losses through recombination pathway k_{CR}.[20] These results have however been questioned by Lewis and co-workers[16,21] who have obtained comparable efficiencies for both Ru- and Os-centered complexes.

We have previously investigated the iodide kinetics in dye-sensitized solar cells assembled using a polymer electrolyte.[15] In this paper, we extend such studies by investigating the kinetic competition between the charge recombination reaction k_{CR} and the regeneration reaction k_{RG} in a variety of controlled conditions (different iodide concentrations, externally applied bias). The experimental approach consists of employing dye-sensitized films as working electrodes in three electrode photoelectrochemical cells to investigate the effect of an externally applied bias on the kinetic competition in the presence of different iodide concentrations. Studies primarily employed the dye *cis*-bis (thiocyanato) bis (2,2′-bypiridine-4,4′-dicarboxylato) ruthenium(II) di(tetrabutylammonium) from here on referred to as $Ru(dcbpy)_2(NCS)_2$. Regeneration kinetics were compared with electrodes sensitized with Zn-tetra-p-carboxy-phenyl-porphyrin (ZnTCPP). Experiments were also carried out in the presence of iodine added to the electrolyte.

Materials and Methods

$Ru(dcbpy)_2(NCS)_2$- and ZnTCPP-sensitized nanocrystalline anatase TiO_2 films were prepared on fluorine-doped SnO_2 glass substrate (LOF TEC 15 glass) as previously described.[22] The film preparation method followed Nazeeruddin et al.[23] (method A), with modifications detailed in ref 24 resulting in approximately 8 μm thick films. Dye sensitization was typically achieved by overnight immersion in a 1.2 mM $Ru(dcbpy)_2(NCS)_2$ solution in a 50:50 acetonitrile:ter-butanol solution. In the case of Zn-tetra-p-carboxy-phenyl-porphyrin, the films were immersed overnight in a 1 mM solution in ethanol. All experiments were carried out at room temperature.

Experiments without external bias were carried out by immersing the dye-sensitized TiO_2 film in an optical cuvette filled with approximately 4 cm^3 of electrolyte solution. Electrolytes were prepared dissolving LiI (99% Aldrich) and $LiClO_4$ (99.99% Aldrich) in anhydrous propylene carbonate (Aldrich). The $LiClO_4$ concentration was adjusted such that all electrolytes had a Li^+ concentration of 0.1 M. This ensured that the effect of lithium cations on the energy levels of the semiconductor remained constant throughout the series of experiments.[14,25,26]

Experiments under bias control employed the dye-sensitized titanium dioxide films as working electrodes in a three electrode photoelectrochemical cell employing a platinum wire counter electrode and an Ag/AgCl reference electrode. Potential control was provided by a home-built potentiostat. The electrolyte was degassed with argon prior to and during all optical experiments in this cell.

Microsecond to millisecond transient absorption spectroscopy was performed as described previously[5] except that the excitation wavelength was set at 620 or 640 nm in the case of $Ru(dcbpy)_2(NCS)_2$ and 560 nm in the case of Zn-tetracarboxy-phenyl-porphyrin. The chosen excitation wavelengths corresponded to sample optical densities of approximately 0.3 in order to avoid nonlinearities in the excitation profile of the sensitized film. The probe wavelength of 800 nm in the case of $Ru(dcbpy)_2(NCS)_2$ and 760 nm in the case of Zn-tetracarboxy-phenyl-porphyrin was chosen with the two monochromators on the tungsten lamp probe beam. In both cases, this probe wavelength monitors induced absorption of dye cations while avoiding absorption bands of the dye ground state. Nanosecond transient absorption spectroscopy was performed with the same laser excitation source and employing a laser diode (Hitachi HL 8325G, 40 mW CW) at 830 nm as probe beam. A fast photodiode and homemade amplifier electronics formed the detector. All transient data were collected employing low-intensity excitation pulses (pulse duration ∼600 ps, ∼25−50 $\mu J/cm^2$, 0.2−2 Hz). These conditions correspond to excitation of ∼1% of the dye molecules per excitation pulse. The effect of applied bias potential on the transient kinetics was reversible. Indistinguishable data were collected at 0 V vs Ag/AgCl prior and after each series of bias-dependent experiments as long as the applied potential did not exceed −0.5 V vs Ag/AgCl. In these conditions, steady state absorption spectra of the samples before and after optical experiments indicated no detectable degradation of the sample during the course of each experiment. Prolonged application of a bias < -0.5 V vs Ag/AgCl led to irreversible changes in the absorption spectra of samples and in the observed kinetics as reported in similar studies in the past and tentatively assigned to dye desorption/degradation.[26,27]

Results

Pulsed optical excitation of $Ru(dcbpy)_2(NCS)_2$-sensitized nanocrystalline TiO_2 films results in a broad absorption increase peaking at ∼800 nm assigned to an absorption band of the $Ru(dcbpy)_2(NCS)_2$ cation.[1] In the absence of redox active species in the electrolyte, this cation state is rereduced by charge recombination with electrons in the semiconductor film (k_{CR}):

$$D^+ + e_{TiO_2} \rightarrow D \qquad (1)$$

Previous studies employing acetonitrile- or ethanol-based electrolytes have demonstrated that this recombination reaction is strongly dependent upon the electrical bias applied to the metal oxide film.[5,26] Analogous behavior was observed for the propylene carbonate-based electrolyte employed in this paper, as illustrated in Figure 2. The recombination dynamics are independent of applied voltage for positive biases but accelerate rapidly at biases <0 mV vs Ag/AgCl.

Figure 3 presents analogous transient absorption data collected in the absence of applied bias but in the presence of different iodide concentrations. The addition of iodide to the electrolyte results in the decay kinetics at 800 nm becoming increasingly biphasic. The faster phase accelerates as a function of increasing iodide concentration. The amplitude of the slower phase increases as the iodide concentration is increased and exhibits a half-life of approximately 0.2−0.5 s independent of iodide concentration. The insert shows an expansion of data collected with the nanosecond setup at early times, indicating that the initial amplitude of the signal, assigned to dye cation formation due to electron injection, is independent of iodide concentration.

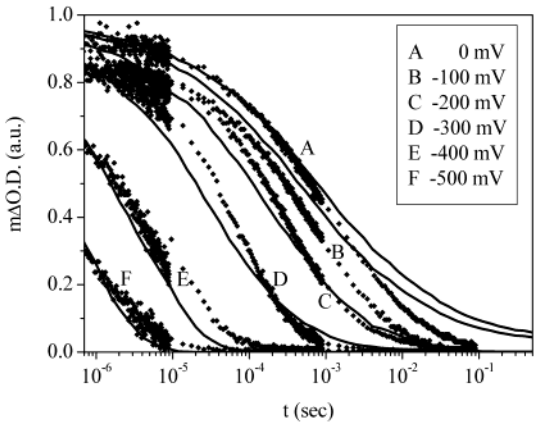

Figure 2. Transient absorption data monitoring the decay of photoinduced absorption of the $Ru(dcbpy)_2(NCS)_2$ cation following pulsed excitation of a dye-sensitized TiO_2 film. Data were collected in a three electrode cell as a function of externally applied bias vs Ag/AgCl applied to the dye-sensitized electrode. The electrolyte was 0.1 M $LiClO_4$ in propylene carbonate. The excitation wavelength was 620 nm, and the signal was probed at 800 nm. Also shown (continuous lines) are numerical calculations of cation state decay using the CTRW model (see text for details).

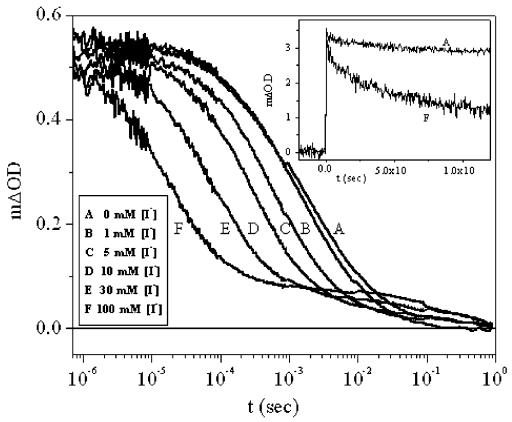

Figure 3. Transient absorption data collected at 800 nm for a $Ru(dcbpy)_2(NCS)_2$-sensitized TiO_2 film measured as a function of iodide concentration. The electrolytes consisted of $LiClO_4$ and LiI in propylene carbonate, with the salt concentration adjusted to maintain a constant Li^+ concentration (0.1 M) and iodide concentrations as indicated in the figure. Also shown is an expansion of data collected at early times for I^- concentrations of 0 and 100 mM.

We have previously suggested that the slow phase observed in the presence of iodide arises from I_2^- absorption.[15] Typical spectral data in support of this suggestion are shown in Figure 4. This figure shows transient spectra collected at 10 μs and 1 ms after excitation of the $Ru(dcbpy)_2(NCS)_2/TiO_2$ films in the presence of 0.1 M I^- ions. The spectrum at 10 μs exhibits the characteristic features of the dye cation state, namely, an absorption bleach centered at ~540 nm (the ground state absorption maximum of the dye) and a broad absorption increase centered at ~800 nm assigned to a dye cation absorption band.[1,28] In contrast, the spectrum at 1 ms remains positive throughout the spectral range studied, with increases in the near-infrared and toward the blue and a minimum at 575 nm. The absence of a negative signal around 500 nm clearly indicates that this spectrum cannot be assigned to dye cation states. The increase in the amplitude of the slow component associated with increasing iodide concentration and with decreasing dye cation lifetime indicates that the spectrum at 1 ms corresponds to long-lived product states generated by the rereduction of the dye cation by iodide ions (k_{RG}). Comparison with literature spectra

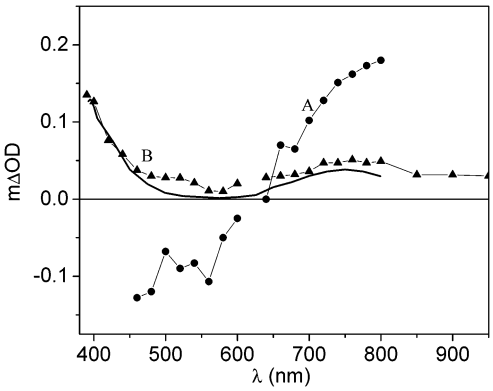

Figure 4. Comparison of the transient absorption spectra measured for a $Ru(dcbpy)_2(NCS)_2$-sensitized film immersed in 0.1 M LiI in propylene carbonate. Spectra are shown at delays of (A) 10 μs and (B) 1 ms after excitation at 620 nm. Also shown (smooth line) is the spectrum of I_2^- determined previously by UV flash photolysis.[29]

indicates that this product state spectra is in good agreement with a spectrum previously assigned in UV flash photolysis experiments to the radical anion state I_2^-,[29,30] as illustrated in Figure 4 (smooth line) in agreement with results we have reported previously employing a polymer electrolyte.[15] These data therefore provide direct support for previous suggestions that iodide reduction of the dye cation results in generation of this species:[13,14]

$$D^+ + 2I^- \rightarrow D + I_2^- \qquad (2)$$

We note that in order to conserve overall charge, the observation of dye cation and I_2^- states implies the concomitant presence of electrons photoinjected into the TiO_2, as has been reported previously by Kay et al.[32] Such injected electrons (e_{TiO_2}) are thought to correspond primarily to localized Ti^{3+} states, known to give rise to a broad absorption increase in the red/near-infrared. It is possible that this Ti^{3+} absorption may also contribute to the positive absorption increase observed for both spectra centered at approximately 800 nm. The extinction coefficient for such Ti^{3+} states is at present controversial.[25,31] Our own studies suggest that under our experimental conditions the extinction coefficient for photoinjected electrons is $\leq 1\,000$ M^{-1} cm^{-1}; absorption by these species is therefore expected to be small relative to those of the dye cation and I_2^- radicals (approximately 6 000 [33] and 2 200 [30] M^{-1} cm^{-1}, respectively). Such e_{TiO_2} probably accounts for the increased photoinduced absorption observed at long wavelengths as compared to the literature spectrum for I_2^- (see Figure 4). In any case, independent of any uncertainty on the extent of Ti^{3+} absorption contributing to the transient data, the long-lived component observed in Figure 3 must be assigned to a long-lived charge separated state generated by the rereduction of the dye cation by the iodide ions.

From the above analysis, we assign the biphasic nature of the decay kinetics observed in the presence of iodide ions to the regeneration reaction k_{RG} (eq 2), resulting in the generation of the long-lived charge-separated product state e_{TiO_2}/I_2^-. At moderate iodide concentrations, kinetic competition occurs between k_{RG} and k_{CR}, resulting in a lower yield of I_2^-. As shown in Figure 3, at iodide concentrations >30 mM, only a small increase in product state yield is observed, indicating that for concentrations ≥30 mM k_{RG} largely dominates over k_{CR} and the yield of I_2^- is close to maximal.

Experiments analogous to those shown in Figures 3 and 4 were repeated for films sensitized with an alternative sensitizer

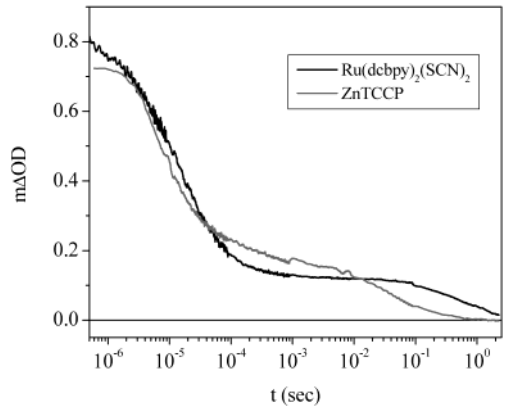

Figure 5. Transient absorption decays observed for $Ru(dcbpy)_2(NCS)_2$ (black)- and ZnTPPC (grey)-sensitized TiO_2 films immersed in 0.1 M LiI in propylene carbonate. In the former case, the excitation and probe wavelengths were 620 and 800 nm, respectively, while in the latter these were 560 and 740 nm.

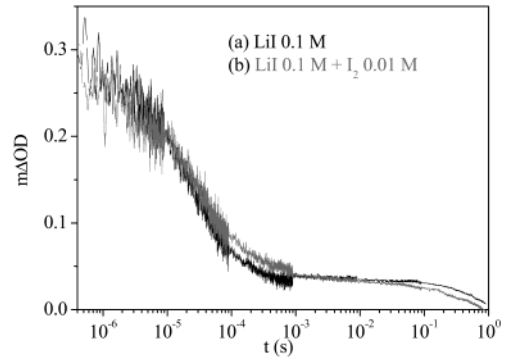

Figure 6. Transient absorption data collected at 800 nm for a $Ru(dcbpy)_2(NCS)_2$-sensitized TiO_2 film measured in the presence of 0.1 M LiI propylene carbonate electrolyte without (a) and with (b) the addition of 0.01 M I_2.

dye, ZnTCPP. We have previously shown that the kinetics of the electron injection k_{inj} and recombination reaction k_{CR} for nanocrystalline TiO_2 sensitized by this dye are essentially indistinguishable from those observed for films sensitized by $Ru(dcbpy)_2(NCS)_2$.[22] Transient absorption kinetics for ZnTCPP/TiO_2 films in the presence of 0.1 M iodide are shown in Figure 5, overlaid on data collected for the $Ru(dcbpy)_2(NCS)_2/TiO_2$ films under the same experimental conditions. Spectra were collected analogous to those shown in Figure 4, showing spectral features of the ZnTCPP cation state at 10 μs and e_{TiO_2}/I_2^- radicals at 1 ms (data not shown). It is apparent that the decay kinetics of the ZnTCPP/$Ru(dcbpy)_2(NCS)_2$ dye cations are similar on the time scale probed, pointing to similar dye regeneration kinetics for these two dyes.

Experiments conducted on $Ru(dcbpy)_2(NCS)_2$-sensitized films in the presence of 0.1 M iodide were further extended by the addition of 0.01 M iodine to the electrolyte. The addition of iodine resulted in no change in the transient data apart from small acceleration of the decay of the slow phase assigned to loss of I_2^- species (Figure 6). The independence of the regeneration reaction on the presence of iodine in solution is in contrast with that observed by Heimer et al.[6] who reported that the addition of 25 mM iodine to 250 mM sodium iodide in propylene carbonate resulted in quenching of up to 90% of the initial dye cation transient signal. The origin of this disagreement is unclear. Our observation indicates that as expected from eq 2, neither iodine nor I_3^- species play a significant role in the dye regeneration kinetics.

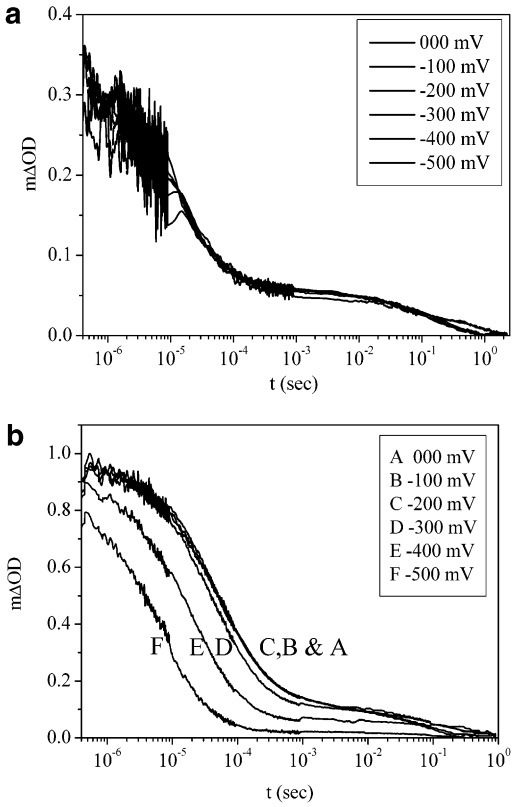

Figure 7. Transient absorption decays observed at 800 nm for $Ru(dcbpy)_2(NCS)_2$-sensitized films as a function of externally applied bias in a three electrode cell using propylene carbonate/$LiClO_4$/LiI electrolytes. The Li^+ concentration was 0.1 M in all cases. Experiments employed iodide concentrations of (a) 0.1 and (b) 0.03 M.

We turn now to experiments as a function of applied bias. Experiments were conducted as for Figure 2 in a three electrode photoelectrochemical cell but with the addition of iodide to the electrolyte. In contrast to the data collected in the absence of iodide ions (Figure 2) and assigned to the recombination reaction k_{CR}, transient data collected in the presence of high concentrations of iodide (0.1 M iodide) were independent of applied bias, with the data being similar to that collected at this iodide concentration in the absence of any applied bias (Figure 3). Typical data are shown in Figure 7a. At this iodide concentration, the dye cation decay kinetics are expected to be dominated by the regeneration reaction k_{RG} (see above). The bias independence of the transient data at these iodide concentrations indicates that k_{RG} is independent of applied electrical bias within the range employed in the experiments.

Kinetic competition between k_{RG} and k_{CR} is expected at more moderate iodide concentrations. Such data are shown in Figure 7b, which shows data collected as a function of applied bias for an iodide concentration of 0.03 M. For potentials > -0.2 V vs Ag/AgCl, the kinetics are independent of applied bias, consistent with the dye cation decay being dominated by the regeneration reaction k_{RG}. However, for potentials ≤ -0.2 V vs Ag/AgCl, an acceleration of dye cation decay kinetics is observed, and the yield of I_2^- species is reduced. This observation is consistent with the expected acceleration of k_{CR} at negative biases resulting in the recombination reaction dominating the decay kinetics at negative applied biases.

Numerical Modeling. The kinetic curves are modeled by Monte Carlo simulation of electron dynamics and cation rereduction following excitation by the laser pulse. This method has been used successfully to model the dye cation recombination kinetics (k_{CR}) in a redox inactive environment.[8] In that case,

electron motion is simulated using a continuous time random walk (CTRW) originally introduced by Scher and Montroll[34] to describe dispersive transport in disordered semiconductors. Electrons move at random on a lattice containing "traps" of variable depth such that the time for each step is determined by the activation energy of the site currently occupied, and site occupancy is limited to satisfy Fermi−Dirac statistics. No long-range forces exist between electrons or electrons and cations, so that dye rereduction is diffusion-limited, occurring whenever an electron moves on to a site occupied by a dye cation.

For the case of an exponential density of trap states,

$$g(E) = \frac{N_t}{k_B T_0} \exp\left(-\frac{(E_C - E)}{k_B T_0}\right) \quad (3)$$

where E_C is the conduction band edge, $k_B T_0$ is the energy coefficient of the exponential, and N_t is the total trap density. The model predicts that the kinetics should follow a "stretched exponential"

$$[D^+(t)] = [D^+(0)] \exp(-n(t/\tau)^\alpha) \quad (4)$$

in the limit where the electron density outnumbers the dye cation density $[D^+]$. Here, τ is a constant and $\alpha = T/T_0$ where T is 298 K. The effective half-life of the cation, $t_{50\%}$, then varies with electron density per cation, n, like

$$t_{50\%} \propto n^{-1/\alpha} \quad (5)$$

The model has been applied to the rereduction kinetics of ruthenium complexes on nanocrystalline TiO_2 and ZnO films in various redox inactive electrolytes, and the behavior predicted by eqs 4 and 5 has been observed in all cases.[9,35,36] We note that this nonlinear dependence of the recombination half-time upon electron density, which we observe experimentally, cannot be explained by alternative second-order, homogeneous models for nongeminate charge recombination.[16]

In the current context, the model must be modified in two respects: (i) the rereduction of D^+ by I^- (eq 2) must be allowed, and (ii) the optical absorbance of the products of this alternative reaction at the probe wavelength must be included.

The regeneration of the dye by I^- is assumed to be first-order in $[D^+]$ and characterized by a rate constant $k(I^-)$, which is some function of $[I^-]$. This assumption requires that $[I^-] \gg [D^+]$ (a condition which is valid in our systems where approximately one dye is excited per nanoparticle, with the possible exception of the lowest iodide concentration) but does not involve any assumption about the order of reaction with respect to $[I^-]$.

During each simulation, one dye cation and n electrons are implanted at random on a lattice inside a spherical shell, which represents the nanoparticle, as in ref 9. Each dye cation is assigned a lifetime with respect to I^- according to

$$\tau_I = -\frac{\ln X}{k(I^-)} \quad (6)$$

where X is a random number between 0 and 1. The electrons perform the random walk, and the simulation stops when either an electron walks on to the cation site (reduction according to eq 1) or the regeneration lifetime τ_I is reached (eq 2), whichever happens first. The cation lifetime and type of event are recorded. Simulations are repeated for 5000 realizations of the lattice for each value of n and $k(I^-)$. The relative dye cation density is compiled from the set of reduction times.

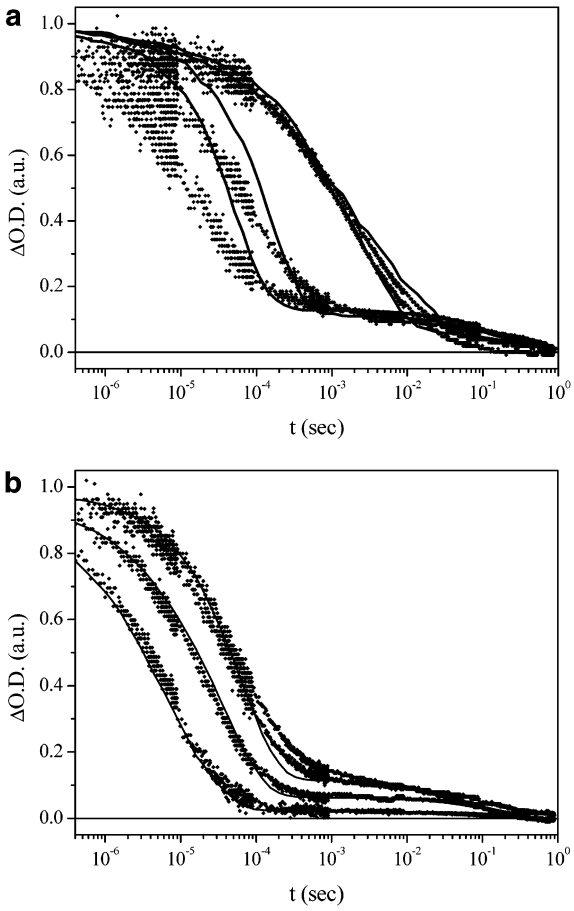

Figure 8. Comparison of experimental transient absorption data at 800 nm (+) with CTRW model calculations (smooth lines) (a) as a function of iodide concentration in the absence of applied bias and (b) as a function of applied bias with an iodide concentration of 0.03 M. Data for panels a and b were taken from Figures 3 and 6b, respectively. (a) Shows data and model calculations for iodide concentrations of 0, 1, 30, and 100 mM and (b) shows data and model calculations for applied bias of −0.3, −0.4, and −0.5 V vs Ag/AgCl in 0.03 M LiI.

The evolution of the absorbing product is due to events of type 2 (dye regeneration by iodide) only. We assume that each regeneration event produces exactly one product species P, assigned above to the charge-separated state e_{TiO_2}/I_2^-. The disappearance of the product is assumed to be second-order, as discussed below. Then, the product density obeys

$$\frac{dP}{dt} = -\frac{d[I^-]}{dt} - k_2 P^2 \quad (7)$$

where k_2 is a constant and the initial condition $P(0) = 0$ applies. P is calculated from the simulation results for $[I^-]$ by numerical integration of eq 7, with k_2 as a fitting parameter. Finally, the relative absorbance of the system is calculated from $[D^+(t)]$ and $P(t)$ by

$$\Delta OD(t) = \Delta OD(0) \times \frac{[D^+(t)] + (\epsilon_P/\epsilon_{D^+})P}{[D^+(0)]} \quad (8)$$

where $(\epsilon_P/\epsilon_{D^+})$ is the ratio of extinction coefficients of product and dye cation. $\Delta OD(t)$ is compared with the experimental optical density relative to its initial value.

To generate $\Delta OD(t)$, the following parameters are required: α, the relationship between n and applied bias, the absolute time scale, the functional form of $k(I^-)$, k_2, and the ratio $(\epsilon_P/\epsilon_{D^+})$.

First, we determine the value of α by fitting the data in the absence of iodide (Figure 2) to a stretched exponential. This yields $\alpha = 0.4 \pm 0.05$. α also yields the relationship between n and applied bias; using eq 5 and observed $t_{50\%}$ values, we estimate that n increases by a factor of about 3 per 100 mV. Note that the bias at which $n = 1$ may vary by up to ±50 mV between samples. Using these values for n (V) and α, we are able to reproduce the kinetics in the iodide free case, as indicated in Figure 2.

To determine the product decay constant k_2 and the ratio ($\epsilon_P/\epsilon_{D^+}$), we analyze the shape of the kinetic curve in the case of a high iodide concentration. Evolution of the product adds a slow tail on to the roughly exponential form of the cation absorbance, much as observed. A best fit is obtained with $k_2 = 5 \times 10^4$ dm^3 mol^{-1} s^{-1} and ($\epsilon_P/\epsilon_{D^+}$) = 0.15. These values are used throughout the simulations. Finally, first- and second-order forms for $k(I^-)$ are evaluated by comparing model predictions with experimental kinetics at different iodide concentrations.

Comparisons of the results of this numerical model with experimental decays are shown in Figure 8. Figure 8a shows the comparison as a function of iodide concentration, and Figure 8b shows the comparison as a function of applied bias at low (0.03 M) iodide concentration. It is apparent that the simulations as a function of applied bias are in good agreement with experimental observations. Comparisons as a function of iodide concentration are in reasonable agreement with a first-order dependence $k(I^-) = k_{RG}[I^-]$, $k_{RG} = 1.6 \times 10^5$ dm^3 mol^{-1} s^{-1}, although it is apparent that this model predicts a somewhat weaker dependence upon iodide concentration than is observed. This deviation will be addressed in detail below.

Discussion

In this paper, we have addressed the electron transfer kinetics of Ru(dcbpy)$_2$(NCS)$_2$-sensitized nanocrystalline TiO$_2$ films as a function of iodide concentration in the electrolyte and electrical potential applied to the TiO$_2$ film. Our experimental observations focus on the decay kinetics of photogenerated dye cations and the formation of product states of the regeneration of dye cations by iodide ions in the electrolyte (k_{RG}) in the presence of different iodide concentrations while controlling the Fermi level in the semiconductor film.

The essential conclusions of our results can be summarized as: (i) A long-lived product state of the iodide reaction with dye cations is observed. The transient spectrum of this state is characteristic of the radical ion I_2^-, and it is therefore assigned to the state e_{TiO_2}/I_2^-. (ii) The rate of iodide regeneration of the dye (k_{RG}) is independent of applied bias and iodine presence in the electrolyte. (iii) Similar regeneration kinetics k_{RG} are observed for two different sensitizer dyes Ru(dcbpy)$_2$(NCS)$_2$ and ZnTCPP. (iv) A numerical model of the dye cation decay in which the charge recombination reaction k_{CR} between dye cations and electrons injected into the metal oxide is modeled as electron diffusion through an exponential distribution of trap states in the metal oxide film and k_{RG} is modeled as a first-order reaction in iodide concentration is in reasonable agreement with experimental observations.

Bias Independence of k_{RG}. The bias independence of k_{RG} is in marked contrast to the strong bias dependence of the recombination reaction k_{CR}. The reaction k_{RG} requires the diffusion of iodide ions to oxidized dye cations adsorbed on the TiO$_2$ film surface. The bias independence of this reaction is consistent with the screening of the surface charge of nanoporous electrode by lithium ions in the electrolyte. Such screening, studied in the absence of applied electric biases, has been addressed in detail elsewhere.[14,37]

Iodide Concentration Dependence of k_{RG}. The rate of the rereduction reaction is expected to be of the form

$$\text{rate} = k_{RG}[D^+][I^-]^x \tag{9}$$

The order x of this reaction with respect to iodide concentration is currently the subject of some controversy.[13,14,16] From eq 2, it is apparent that a second-order behavior in iodide concentration might be expected. Alternatively, it has been suggested that a reaction pathway involving formation of an I$^\bullet$ radical intermediate would yield first-order kinetics in iodide concentration[13] or that the reaction proceeds through the formation of (dye$^+$/I$^-$) and/or (I$^-$/I$^-$) ion pairs on the semiconductor surface.[14] The order of the reaction with respect to iodide concentration has been shown to be first-order,[13] although the range of iodide concentrations ($0-10^{-4}$ M) investigated was limited. It is apparent from Figure 3 that an increase in the iodide concentration from 1 to 100 mM results in an approximately 100-fold increase in the rate of dye cation decay, consistent with first-order behavior. More quantitatively, our numerical model, assuming first-order behavior in iodide concentration, provides a reasonable fit to these data. We note that this model somewhat underestimates the iodide concentration dependence of the dynamics. However, a significantly worse fit is obtained if second-order behavior is assumed and we conclude that the reaction is close to first-order with respect to iodide concentration.

The rate constant that we obtain for the regeneration reaction from our numerical modeling is $k_{RG} = 1.6 \times 10^5$ dm^3 mol^{-1} s^{-1}. This rate constant is of similar magnitude to values recently reported by Pelet et al.[14] and Kuciauskas et al.[16] although significantly smaller than those reported by Heimer et al. ($>2 \times 10^7$ dm^3 mol^{-1} s^{-1})[6] and Kamat et al. (1.2×10^{10} dm^3 mol^{-1} s^{-1}).[13]

At high iodide concentrations, our transient absorption experiments are conducted in the limit $[D^+] \ll [I^-]$. Under these conditions, the iodide concentration is constant, and the overall regeneration reaction order is expected to be pseudofirst-order, independent of the reaction order with respect to iodide ($k_{eff} = k_{RG}[I^-]^x$). If the regeneration dynamics are homogeneous throughout the film, as assumed in our numerical modeling, a monoexponential decay of the dye cation is therefore expected. It is however apparent from Figures 3 and 8a that this is not the case. To address the origin of this nonexponential behavior, the regeneration dynamics were studied as a function of dye coverage. Fillinger and Parkinson[38] have suggested the onset of a cation-hopping mechanism in Ru(dcbpy)$_2$(NCS)$_2$-sensitized TiO$_2$ films at dye coverages exceeding 30%, resulting in the dye cation produced by electron injection migrating among adjacent sensitizer molecules, potentially complicating the observed regeneration dynamics. However, we observed indistinguishable dynamics at high and low (~10 and ~100%) dye coverages (data not shown), indicating that such hopping dynamics are not important for consideration of the regeneration dynamics reported here. Alternatively, this nonexponential behavior may derive from inhomogeneity in the energetics of the regeneration reaction, consistent with our recent modeling[39] of nonexponential injection kinetics for this experimental system in terms of a distribution of free energies for the injection step.

Previous studies on dye-sensitized colloids[12] have suggested that complex formation between Ru(dcbpy)$_3$ and iodide ions may enhance the rate of iodide rereduction of the dye cation. Our experiments provide no evidence for such complex formation, in agreement with subsequent work.[6,13,14] Our observation of similar rereduction kinetics for two different dyes—

$Ru(dcbpy)_2(NCS)_2$ and ZnTCPP—is also not readily reconciled with specific dye/iodide complex formation. We note in this regard that both dyes employed exhibit similar oxidation potentials in solution. Studies with alternative dyes with less positive oxidation potentials result in significantly lower I_2^- product yields (Clifford, J.; Durrant, J. R. Unpublished data), consistent with recent comparisons of the function of osmium and ruthenium sensitizer dyes.[21]

Decay of I_2^- Product Species. In the presence of iodide, a long-lived transient absorption signal is observed, exhibiting a half-time of approximately 0.2−0.5 s. This signal is assigned primarily to I_2^- absorption of the charge-separated state e_{TiO_2}/I_2^-. The decay of this signal is independent upon electrically applied bias (see Figure 7), suggesting that this decay cannot be assigned to charge recombination between electrons in the semiconductor (e_{TiO_2}) and I_2^-.

$$e_{TiO_2} + I_2^- \rightarrow 2I^- \quad (10)$$

We assign this decay to the I_2^- dismutation reaction:

$$2I_2^- \rightarrow I^- + I_3^- \quad (11)$$

The I_3^- will presumably subsequently decay by charge recombination with e_{TiO_2}, although neither species can be observed unambiguously in the experiments we report here. In analogous experiments employing an iodide/iodine-based polymer electrolyte, the decay of the signal was observed to accelerate rapidly under continuous white light illumination.[15] This acceleration is consistent with assignment of this signal to the dismutation reaction, with the white light illumination resulting in the steady state accumulation of I_2^- species in the polymer electrolyte and faster decay kinetics as a result.

The rate constant k_2 for this dismutation reaction is determined to be 5×10^4 dm^3 mol^{-1} s^{-1} as detailed above. The slow rate of the dismutation reaction ($t_{1/2} \sim 0.2-0.5$ s) observed under our experimental conditions is remarkable and attributed in part to the low concentration of I_2^- generated by the low energy laser excitation. We note that assuming that the reaction is diffusion-controlled, literature diffusion constants for analogous species such as I_3^- would yield a significantly higher dismutation rate constant than that observed here. This finding suggests that the diffusion of I_2^- radicals within the film pores may be impeded by interactions with the film surface. This conclusion is consistent with a recent study, which suggested that the diffusion constant for the analogous species I_3^- is approximately 10-fold smaller within the film pores relative to bulk solution.[40] We further note the rate constant k_2 for this dismutation reaction is of similar magnitude to that of the regeneration reaction k_{RG}, which may be indicative of both reactions being rate-limited by the diffusion of iodide species within the film pores.

Implications for Solar Cell Function. The voltage output of dye-sensitized solar cells is primarily limited by the acceleration of interfacial recombination reactions as the Fermi level and therefore the electron density of the nanocrystalline TiO_2 film is raised. Two recombination reactions are possible; injected electrons may recombine either with oxidized dyes (k_{CR} in Figure 1) or with oxidized redox couple. In this paper, we addressed directly for the first time the kinetic competition between k_{CR} and the desired regeneration reaction k_{RG} as a function of the voltage applied to the TiO_2 film. We find that in contrast to the recombination reaction k_{CR}, the regeneration reaction is independent of applied voltage. Kinetic competition between k_{CR} and k_{RG} is observed to be important for moderate iodide concentrations (30 mM), resulting in a significant loss in the yield of k_{RG} as the TiO_2 Fermi level is raised to levels comparable to V_{oc}, the cell open circuit voltage. However, for higher iodide concentrations, we find $k_{RG} > k_{CR}$ for all applied voltages, suggesting that in liquid electrolyte devices employing such iodide concentrations, charge recombination between injected electrons and oxidized dye species will not be a significant loss mechanism limiting device performance. This conclusion is consistent with previous frequency domain analyses of device performance, which have indicated that the primary recombination loss mechanism in liquid electrolyte devices is between injected electrons and oxidized species in the electrolyte (I_3^- ions)[41,42] However, extensive studies are currently under way to develop alternative electrolytes, including polymer electrolytes and molten salts. In such alternative electrolytes, the slower iodide diffusion dynamics may result in kinetic competition between k_{CR} and k_{RG} being a more significant loss mechanism limiting device performance.

Studies of charge recombination between injected electrons and oxidized redox electrolyte have generally only considered recombination with I_3^- species.[41,43] We note that the remarkably slow dismutation rate for I_2^- species reported here may result in accumulation of this species in functioning devices, an issue not considered previously in models of device function.

Acknowledgment. Thanks are due to Dr. C. J. Barnett and R. Monkhouse for assistance on the electronic data collection and processing, to Dr. D. R. Klug for helpful discussions and preliminary measurements on his flash photolysis apparatus, and Dr. J. Moser of EPFL Lausanne for valuable discussions. Thanks are due to John N. Clifford for help with the collection of nanosecond data. I.M. performed the work presented here while a Marie Curie Fellow of the European Union. Financial support from the EPSRC is also gratefully acknowledged.

References and Notes

(1) Tachibana, Y.; Moser, J. E.; Grätzel, M.; Klug, D. R.; Durrant, J. R. *J. Phys. Chem. B* **1996**, *100*, 20056−20062.
(2) Asbury, J., B.; Ellingson, R., J.; Ghosh, H., N.; Ferrere, S.; Nozik, A. J.; Lian, T. *J. Phys. Chem. B* **1999**, *103*, 3110−3119.
(3) Tachibana, Y.; Haque, S. A.; Mercer, I. P.; Moser, J. E.; Klug, D. R.; Durrant, J. R. *J. Phys. Chem. B* **2001**, *105*, 7424−7431.
(4) Kallioinen, J.; Lehtovuori, V.; Myllyperkiö, P.; Korppi-Tommola, J. *Chem. Phys. Lett.* **2001**, *340*, 217−221.
(5) Haque, S. A.; Tachibana, Y.; Klug, D. R.; Durrant, J. R. *J. Phys. Chem. B* **1998**, *102*, 1745−1749.
(6) Heimer, T. A.; Heilweil, E. J.; Bignozzi, C. A.; Meyer, G. J. *J. Phys. Chem. A* **2000**, *104*, 4256−4262.
(7) O'Regan, B.; Moser, J. E.; Anderson, M.; Grätzel, M. *J. Phys. Chem.* **1990**, *94*, 8720−8726.
(8) Nelson, J. *Phys. Rev. B* **1999**, *59*, 15374−15380.
(9) Nelson, J.; Haque, S. A.; Klug, D. K.; Durrant, J. R. *Phys. Rev. B* **2001**, *63*, 205321.
(10) Bach, U.; Lupo, D.; Comte, P.; Moser, J. E.; Weissörtel, F.; Salbeck, J.; Spreitzer, H.; Grätzel, M. *Nature* **1998**, *395*, 583−585.
(11) Nogueira, A.-F.; De Paoli, M.-A.; Durrant, J. R. *Adv. Mater.* **2001**, *13*, 826−830.
(12) Fitzmaurice, D. J.; Frei, H. *Langmuir* **1991**, *7*, 1129−1137.
(13) Nasr, C.; Hotchandani, S.; Kamat, P. V. *J. Phys. Chem. B* **1998**, *102*, 4944−4951.
(14) Pelet, S.; Moser, J. E.; Grätzel, M. *J. Phys. Chem. B* **2000**, *104*, 1791−1795.
(15) Nogueira, A.-F.; De Paoli, M.-A.; Montanari, I.; Monkhouse, R.; Nelson, J.; Durrant, J. R. *J. Phys. Chem. B* **2001**, *105*, 7517−7524.
(16) Kuciauskas, D.; Freund, M. S.; Gray, H. B.; Winkler, J. R.; Lewis, N. S. *J. Phys. Chem. B* **2001**, *105*, 392−403.
(17) Moser, J. E.; Grätzel, M. *Helv. Chim. Acta* **1982**, *65*, 1436−1444.
(18) Henglein, A. *Ber. Bundes. Phys. Chem.* **1982**, *86*, 241−246.
(19) Fitzmaurice, D. J.; Eschle, M.; Frei, H.; Moser, J. *J. Phys. Chem.* **1993**, *97*, 3806−3812.
(20) Alebbi, M.; Bignozzi, C. A.; Heimer, T. A.; Hasselmann, G. M.; Meyer, G. J. *J. Phys. Chem. B* **1998**, *102*, 7577−7581.

(21) Sauvé, G.; Cass, M. E.; Coia, G.; Doig, S. J.; Lauermann, I.; Pomykal, K. E.; Lewis, N. S. *J. Phys. Chem. B* **2000**, *104*, 6821−6836.

(22) Tachibana, Y.; Haque, S. A.; Mercer, I. P.; Durrant, J. R.; Klug, D. R. *J. Phys. Chem. B* **2000**, *104*, 1198−1205.

(23) Nazeeruddin, M. K.; Kay, A.; Rodicio, I.; Humphry-Baker, R.; Mueller, E.; Liska, P.; Vlachopoulos, N.; Graetzel, M. *J. Am. Chem. Soc*. **1993**, *115*, 6382−6390.

(24) Topoglidis, E.; Lutz, T.; Willis, R. L.; Barnett, C. J.; Cass, A. E. G.; Durrant, J. R. *Faraday Discuss.* **2000**, *116*, 35−46.

(25) Redmond, G.; Fitzmaurice, D. *J. Phys. Chem.* **1993**, *97*, 1426−1430.

(26) Haque, S. A.; Tachibana, Y.; Willis, R. L.; Moser, J. E.; Grätzel, M.; Klug, D. R.; Durrant, J. R. *J. Phys. Chem. B* **2000**, *104*, 538−547.

(27) Lemon, B. I.; Hupp, J. T. *J. Phys. Chem. B* **1999**, *103*, 3797−3799.

(28) Moser, J. E.; Noukakis, D.; Bach, U.; Tachibana, Y.; Klug, D. R.; Durrant, J. R.; Humphry-Baker, R.; Gratzel, M. *J. Phys. Chem. B* **1998**, *102*, 3649−3650.

(29) Devonshire, R.; Weiss, J. J. *J. Phys. Chem.* **1968**, *72*, 3815.

(30) Hug, G. L. *Natl. Stand. Ref. Data Ser. U.S. Natl. Bur. Stand.* **1981**, *69*, 541.

(31) Rothenberger, G.; Fitzmaurice, D.; Grätzel, M. *J. Phys. Chem.* **1992**, *96*, 5983−5986.

(32) Kay, H.; Humphrey-Baker, R.; Grätzel, M. *J. Phys. Chem.* **1994**, *98*, 952−959.

(33) Tachibana, Y. Charge Separation and Recombination in Dye Sensitised Semiconductor Solar Cells, Ph.D. Thesis, Imperial College, 2000.

(34) Scher, H.; Montroll, E. W. *Phys. Rev. B* **1975**, *12*, 2455−2477.

(35) Willis, R. L.; Olson, C.; O'Regan, B.; Lutz, T.; Nelson, J.; Durrant, J. R. *J. Phys. Chem. B* **2002**, *106*, 7605−6713.

(36) Biswas, A. M.; Haque, S. A.; Lutz, T.; Montanari, I.; Olson, C.; Willis, R. L.; Durrant, J. R. *Charge Recombination and Transport in Dye Sensitised TiO_2 Photovoltaic Devices*; XXVIII IEEE Photovoltaic Specialist Conference 2000, Anchorage, Alaska, 2000.

(37) Zaban, A.; Meier, A.; Gregg, B. A. *J. Phys. Chem. B* **1997**, *101*, 7985−7990.

(38) Fillinger, A.; Parkinson, B. A. *J. Electrochem. Soc*. **1999**, *146*, 4559−4564.

(39) Tachibana, Y.; Rubtsov, I. V.; Montanari, I.; Yoshihara, K.; Klug, D. R.; Durrant, J. R. *Photochem. Photobiol., A* **2001**, *142*, 215−220.

(40) Kebede, Z.; Lindquist, S.-E. *Sol. Energy Mater. Sol. Cells* **1998**, *51*, 291−303.

(41) Huang, Y.; Schlichthörl, G.; Nozik, A. J.; Grätzel, M.; Frank, A. J. *J. Phys. Chem. B* **1997**, *101*, 2576−2582.

(42) Duffy, N. W.; Peter, L. M.; Rajapakse, R. M. G.; Wijayantha, K. G. U. *J. Phys. Chem. B* **2000**, *104*, 8916−8919.

(43) Ferber, J.; Stangl, R.; Luther, J. *Sol. Energy Mat. Sol. Cells* **1998**, *53*, 29−54.